A Miniaturized Reverse Electrodialysis-Powered Biosensor Using Electrochemiluminescence on Bipolar Electrode

Seol Baek, Seung-Ryong Kwon, Song Yi Yeon, Sun-Heui Yoon, Chung Mu Kang, Seok Hee Han, Dahye Lee, and Taek Dong Chung

Anal. Chem., **Just Accepted Manuscript** • DOI: 10.1021/acs.analchem.7b05425 • Publication Date (Web): 09 Mar 2018

A Miniaturized Reverse Electrodialysis-Powered Biosensor Using Electrochemiluminescence on Bipolar Electrode

Seol Baek[1,‡] , Seung-Ryong Kwon[1,‡], Song Yi Yeon[1], Sun-Heui Yoon[1], Chung Mu Kang[2], Seok Hee Han[1], Dahye Lee[1], and Taek Dong Chung[1,2,*]

[1]Department of Chemistry, Seoul National University, Seoul 08826, Korea.

[2]Advanced Institutes of Convergence Technology, Suwon-Si, Gyeonggi-do 16229, Korea.

* Corresponding author. Tel.: +82-2-880-4362. Fax: +82-2-887-4354; E-mail: tdchung@snu.ac.kr

ABSTRACT: We suggest electrochemiluminescence (ECL) sensing platform driven by eco-friendly, disposable, and miniaturized reverse electrodialysis (RED) patches as an electric power source. The flexible RED patches composed of ion-exchange membranes (IEMs) can produce voltage required for ECL sensing by simply choosing the appropriate number of the IEMs and the ratio of salt concentrations. We integrate the RED patch with a bipolar electrode on the microfluidic chip to demonstrate the proof-of-concept, i.e. glucose detection in the range of 0.5 - 10 mM by observing ECL emissions with naked eyes. The miniaturized RED-powered biosensing system is widely applicable for electrochemical sensing platforms. This is expected to be a solution for practical availability of battery-free electrochemical sensors for disease diagnosis in developing countries.

Bipolar electrochemistry involves no direct electrical contact to bipolar electrodes (BPEs). When a BPE, an electric conductor, lies on a microfluidic chip channel filled with an ionic solution and a sufficient external voltage is introduced through two driving electrodes, faradaic reactions occur at the lateral ends of the BPE.[1] To date, various applications of bipolar electrochemistry have been developed, e.g. material fabrication,[2] sensing,[3] screening,[4] enrichment,[5] and separation[6]. In particular, electrochemiluminescence (ECL)-based bioanalysis is one of the most powerful analytical tools when coupled with bipolar electrochemistry. This is because ECL signals can provide direct information about not only the magnitude of the current passing through a BPE but also the quantity of analytes present on the BPE surface.[3,7-11] However, many challenges still remain in developing practical analytical devices. For example, paper-based BPEs applicable in the third world and developing countries have recently been reported for disease diagnosis, but they still require external power sources to drive electrochemical reactions on their surfaces.[11,12] Therefore, an inexpensive, eco-friendly, and easy-to-use power source is the most essential requirement for the practical use in those countries. In this respect, we introduce a biomarker-sensing device integrated with a miniaturized patch-type reverse electrodialysis (RED) system for the first time.

RED, a non-polluting technology generating electric power, has drawn a keen attention because it exploits inexhaustible salt gradients (e.g. seawater and river water at estuaries) as energy resources.[13] When anion exchange membranes (AEMs) and cation exchange membranes (CEMs) are alternatively stacked and two salt solutions in different concentrations are brought into contact through ion exchange membranes (IEMs), a potential develops over each IEM. About 80 mV can be obtained through a single IEM under a salinity ratio of 30 (i.e. 0.017 and 0.50 M NaCl solutions) on the assumption of the perfect permselectivity. Thus, an RED system can provide any voltage by simply selecting the number of IEMs and a salinity ratio. In this work, we manufactured miniaturized RED patches as eco-friendly disposable power sources for the operation of ECL-reporting electrochemical sensors. The electric power generated from the patch-type RED drives the ionic circuit that develops electrochemical potential gradient over a BPE on a microfluidic chip. In the ionic circuit, charge carriers are ions without the need of any electronics, e.g. metal electrodes (e.g. Ag/AgCl and Pt), resistors, capacitors and so on. As for the sensing devices powered by normal electric sources, ideally *non-polarized* electrode such as Ag/AgCl is essential to minimize the impedance, thus voltage drop, at the interface. Inconvenience of conventional *non-polarized* electrodes causes most of small sensors including microfluidic system to adopt bare metal electrodes, novel metals in many cases, to transmit electricity between the electric power source and electrolyte medium. As a result, voltage of low frequency must involve faradaic reactions at the electrode interface, producing electric impedance that reduces the voltage applied to electrolyte solution. The proposed system in this work avoids both voltage drop and faradaic reaction, while allowing sensing devices exempt from novel metal electrodes, i.e. Pt, Ag, and Au.[10,14]

To combine a microfluidic chip with the RED patch for biosensing applications, we fabricated several types of RED patches. Then, we systematically analyzed electrical properties of the RED patches to find the optimal condition for microfluidic sensors that consist of a long indium-tin-oxide (ITO) electrode in a microchannel (**Scheme 1**). Quantifying ECL emissions on the ITO BPE with respect to the potential applied by a potentiostat first, we compared them with those induced by the RED patch. Finally, the RED-powered microfluidic system was

Scheme 1. Schematic Design of the RED-Powered Biosensing System

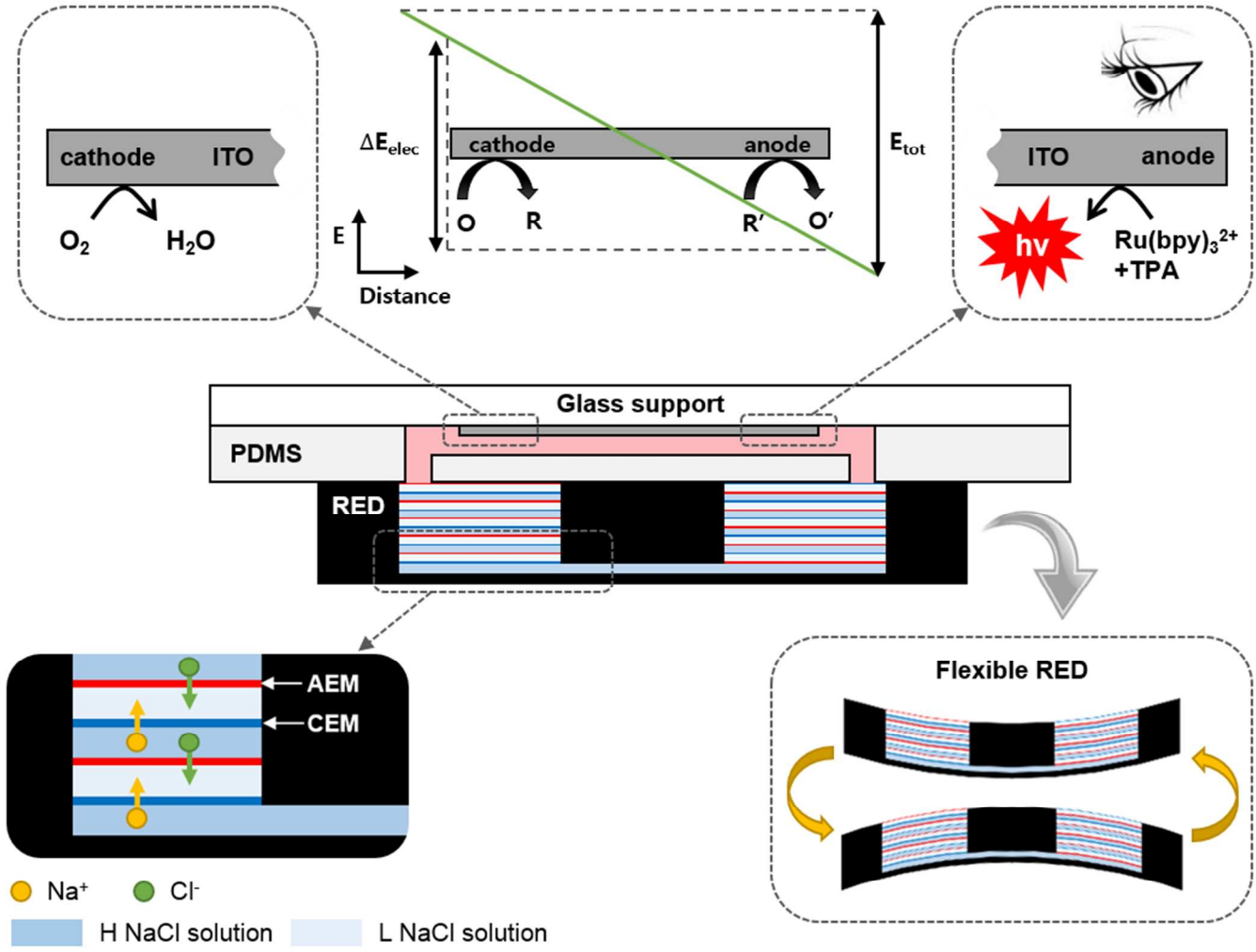

used for the naked eye detection of glucose to demonstrate biosensor applicability.

EXPERIMENTAL SECTION

Chemicals and Materials. Tris(2,2'-bipyridyl)dichlororuthenium(II) hexahydrate ($Ru(bpy)_3Cl_2 \cdot 6H_2O$), tripropylamine (TPA), D-(+) glucose, glucose oxidase (GO_x) from aspergillus niger (163,400 units/g) and indium-tin-oxide (ITO) coated (surface resistivity 8-12 Ω/square) glass slide were purchased from Sigma-Aldrich (USA). Polydimethylsiloxane (PDMS) monomer and curing agent were bought from Dow Corning (Midland, MI, USA). Selemion CMV (cation exchange membrane) and AMV (anion exchange membrane) were bought from Asahi Glass Co., Ltd. (Japan). Waterproof double-sided tape (ACE CROSS SBX) was purchased from Koyo-kagaku Co. Ltd. (Japan). ECL solution was prepared in 0.1 M phosphate buffered saline (PBS, pH 6.9) containing 5 mM $Ru(bpy)_3^{2+}$ and 25 mM TPA. All aqueous solutions were prepared using deionized water (18.2 MΩ/cm, Barnstead Nanopure Diamond System).

Fabrication of RED Patch. A typical RED patch in our study was designed as shown in **Scheme 1 and Figure S1.** CEMs and AEMs were stacked alternately in parallel two columns. Double-sided waterproofing tape (4.0 × 2.0 cm^2, thickness: 250 μm/layer), which had two square holes (1.0 × 1.0 cm^2) in distance of 1.0 cm between them, was used as a frame. A CEM and an AEM were attached over each hole of the double-sided water proofing tape. We put two-superimposed nonconductive fabric spacers (1.0 × 1.0 cm^2) on the ion exchange membrane to make them fit into the hole of upper double-sided waterproofing tape layer. Sterile hypodermic needles (22G) were placed on the spacers for the injection of saline solutions. The unit layer of double-sided waterproofing tape, CEM, AEM, spacers, and hypodermic needles was repeated as many times as desired, while only ion exchange membranes were stacked alternatively. On the uppermost floor, three-layered double-sided waterproofing tape that had a rectangular hole (3.0 × 1.0 cm^2) inside was attached and a rectangular spacer (3.0 × 1.0 cm^2) was laid inside this hole. Finally, an overhead projector film (4.0 × 2.0 cm^2) covered the top of the RED patch. For operating the RED patch as a power source, we used 4.4 M and 0.011 M NaCl solutions as a highly and a low concentrated saline solution, respectively. We alternately

injected these two-different concentrated NaCl solutions between the layers through needle where the uppermost floor was always filled with a high concentrated solution for low solution resistance.

Fabrication of Microfluidic Chip and ITO BPE. A microfluidic chip consists of a PDMS channel and an ITO-coated glass slide. The PDMS channel (length: 2.4 cm, width: 1.0 mm, depth: 50 μm) was combined with the glass slide to contain the ITO BPE (length: 2.2 cm, width: 5.0 mm) in the channel. At the ends of the channel, holes (diameter: 3 mm) for reservoirs were punched through the PDMS chip. The PDMS chip and the ITO BPE were fabricated as follows. To manufacture the PDMS channel, a silicon wafer was cleaned with piranha solution (H_2SO_4 and H_2O_2 with a ratio of 3 : 1) and deionized water, followed by dehydration baking (150 °C, 15 min). SU-8 3025 photoresist was spin-coated (500 rpm for 5 s and 1700 rpm for 30 s in sequence) on the Si wafer, and prebaked on a hot plate (95 °C, 20 min). We let the Si wafer exposed to UV light (21 mJ/cm^2, 15 s) through a photomask and baked at 65 °C for 1 min and 95 °C for 4 min, respectively, before developing a photoresist pattern. The mixture of PDMS base and curing agent (10 : 1) was poured onto the PDMS mold as prepared, degassed under vacuum, and cured at 80 °C for 1.5 h.

ITO BPEs were fabricated by a wet-etching process. First of all, we prepared a clean ITO-coated glass slide by washing with ethanol, acetone, and deionized water in order. Hexamethyldisilazane (HMDS) was spin-coated on the ITO surface and baked on a hot plate at 120 °C for 1.5 min. Then, photoresist (AZ 4620) was also spin-coated and baked at 100 °C for 1.5 min. We illuminated UV light on the photoresist layer through a mask pattern. Next, a photoresist pattern was developed using AZ400K developer and baked at 120 °C for 13 min. The bare ITO surface was etched with TIN etchant (TE-100) while preserving the patterned ITO, which covered with the photoresist pattern. The remaining photoresist was removed with acetone under sonication. The ITO BPE was washed with deionized water. Finally, we used oxygen plasma to activate the surfaces of the PDMS chip and the glass slide with the BPE for making them bound permanently.

Measurement of Microchannel Resistance. The PDMS microchannel in the same dimension of the BPE-containing microfluidic chip was prepared and combined with a bare glass slide. After filling the microchannel with 0.1 M phosphate buffered saline, we configured a circuit consisting of the microchannel and a resistor with a known value, 1.01 MΩ for the measurement of microchannel resistance (**Figure S3**). We placed two Ag/AgCl electrodes at the ends of the microchannel to minimize resistance of charge transfers. The voltage drop over the resistor was recorded as 0.758 V while we applied a certain voltage, 1.0 V into this circuit, thereby estimating microchannel resistance according to the following equation (voltage division rule).

$$R_{\mathrm{ch}} = R_{\mathrm{known}} \times \frac{V_{\mathrm{ch}}}{V_{\mathrm{re}}} = 1.01\ \mathrm{M\Omega} \cdot \frac{(1-0.758)\ \mathrm{V}}{0.758\ \mathrm{V}} = 322\ \mathrm{k\Omega} \quad (1)$$

where R_{ch} is the microchannel resistance, R_{known} is the external resistor with a known value (1.01 MΩ), V_{ch} is the voltage drop occurred across the microchannel, and V_{re} is the voltage drop occurred across the external resistor.

Electrochemical Measurement in Conventional Three-Electrode System. The electrochemical measurement of ECL reaction was performed using a CHI660A electrochemical workstation (CH Instruments, USA). An electrochemical cell for a three-electrode system was filled with 5 mM $Ru(bpy)_3^{2+}$ and 25 mM TPA in 0.1 M PBS solution (pH 6.9). A bare ITO (0.2 cm^2) as working electrode, a platinum counter, and an Ag/AgCl (3 M NaCl) reference were used for the electrochemical experiments. Typical linear sweep voltammograms were recorded at the scan rate of 0.05 V/s.

Detection of Glucose Using ECL. To fabricate glass-based microfluidic chips, we prepared etched glass slides with a depth of 50 μm by conventional wet-etching process.[15] Microchannel in the glass slide was separated into two parts (i.e. sensing and reporting parts) by 4 mm, which had two rectangles with a dimension of 1.1 cm in length and 1.0 mm in width (**Figure 4a**). Four holes (1.5 mm in diameter) at the ends of each channel were drilled in the glass slide for solution reservoirs. Then, the etched glass slide was attached to the patterned ITO BPE coated glass slide as follows. Two glasses were immersed in the solution of 2:2:1 (v/v) NH_4OH (30%) / H_2O / H_2O_2 (30%) for 1 h at 180 °C. After rinsing with deionized water and washing with alkonox detergent, we attached two glass slides to each other by pressure. Checking that no solution remained on glasses, we confirmed the status of microchannel in the glass chip.

For an ECL measurement, 30 μL of ECL solution and 30 μL of glucose and glucose oxidase (1 mg/mL) in PBS solution (pH 6.9) were injected into the reporting channel and the sensing channel, respectively. Then, we incubated this channel for 30 min at room temperature to allow the enzymatic reactions for H_2O_2 generation before capturing ECL images.

Bipolar Electrochemistry and ECL Image Analysis. We applied a constant voltage to the ends of the microchannel through Ag/AgCl driving electrodes using a potentiostat (IviumStat electrochemical workstation, USA). ECL images were taken with an exposure time of 15 s in a dark room using a digital camera (Canon EOS 750D, ISO 6400). ECL intensities from the images were analyzed by using the ImageJ software. To construct a calibration curve for glucose, we measured all ECL intensities based on the same area, which is at least larger than the ECL-emissive area for 10 mM glucose. All quantified ECL intensities were then normalized to the highest level (i.e. 10 mM).

For the integration of the RED patch with the BPE-microfluidic chip, we aligned the membranes of the RED patch to contact with the two-end reservoirs of the microfluidic chip (**Scheme 1 and Figure S2**). Immediately after injection of NaCl solutions, an ECL image was captured to be analyzed by the ImageJ software.

RESULTS AND DISCUSSION

Characterization of the Miniaturized RED Patches and the Microfluidic Chip. The miniaturized RED patches in this work have two parallel columns, i.e. the stacks of ion-selective membranes, to make themselves integrated with a microfluidic chip (**Scheme 1 and Figure S1**). Injection of NaCl solutions into an RED patch immediately gives voltage as a function of the salinity ratio and the number of IEMs. Theoretically, the voltage generated across an IEM is estimated to be about 155 mV with a salinity ratio of 400 (4.4 and 0.011 M NaCl) on the assumption of 100% permselectivity of the IEMs. As an example, the RED patch with 10 pairs of IEMs generates an ini-

tial voltage of 2.50 V, which is 89% of the theoretical value (i.e. 2.80 V). This difference mostly stems from imperfect permselectivity of the IEMs. Nevertheless, the initial voltage of the RED patches is directly proportional to the number of IEM pairs up to 3.7 V (R^2 = 0.99) (**Figure 1a**). Similar to the voltage responses, the resistance of the RED patches also shows a linear relationship to the number of IEM pairs (R^2 = 0.99) (**Figure 1b**). Most of the resistance is attributed to the IEMs and 0.011 M NaCl solutions, while the resistance of 4.4 M NaCl solutions should be negligible because of much higher electrical conductivity.[16] We compared the resistance of the RED patches with that of the microchannel (length: 2.4 cm, width: 1.0 mm, depth: 50 μm). The measured resistance of the microchannel is 322 kΩ, which is 554, 476, and 409-fold higher than that of the 8, 10, and 12-layered RED patches, respectively. Thus, almost the entire voltage generated from the REDs is applied to the microchannel.

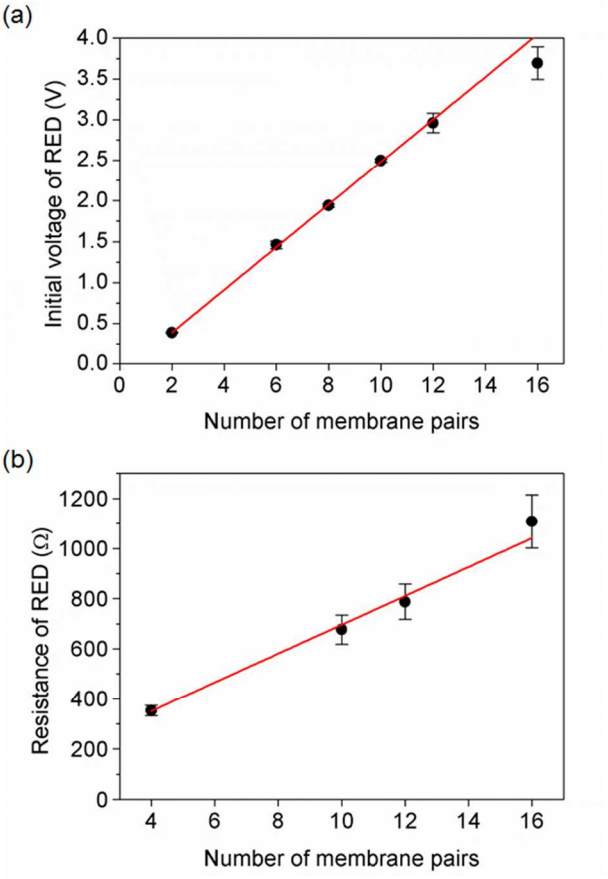

Figure 1. Electrical characterization of RED patches. The initial voltage of RED patches immediately after injection of 0.011 and 4.4 M NaCl solutions (a) and the resistance of RED patches (b) as a function of the number of IEM pairs.

ECL in a Three-Electrode System. To predict an onset potential of ECL reactions on the BPE in the microfluidic chip, we performed electrochemical measurements in a three-electrode system using a macro ITO (surface area of 0.2 cm^2) as a working electrode. In the presence of 5 mM $Ru(bpy)_3^{+2}$ and 25 mM TPA in 0.1 M PBS solution (pH 6.9), an oxidative current apparently appears from 0.45 V and greatly increases after 0.9 V, while there is little change in current under the PBS-only condition (**Figure S4a**). On the other hand, the current responses in the reductive sweep are similar regardless of the presence of $Ru(bpy)_3^{2+}$ and TPA in PBS solution. The cathodic current substantially increases at more negative than -0.7 V, which is attributed to oxygen and water reduction (**Figure S4b**).[17] In the principle of the bipolar electrochemistry, oxidative and reductive currents passing through the BPE in the microchannel must be equal when faradaic reactions occur ($i_c = -i_a$). According to the linear sweep voltammograms, the difference between the cathodic and anodic potentials at a given current density of ± 50 μA/cm^2 was calculated as

$$\Delta E_{elec} = E_c - E_a = 1.049 - (-0.846) = 1.895 \text{ V} \quad (2)$$

This indicates that we need a potential difference larger than 1.895 V between the two ends of the BPE to observe an apparent ECL emission.

ECL on the BPE in the Microfluidic Channel. We systematically analyzed ECL intensities with respect to applied voltages to two driving Ag/AgCl electrodes positioned at the ends of the microchannel. *Non-polarizable* Ag/AgCl electrodes minimize potential drops at the interface so that as large and accurate voltage as possible should be applied along the microchannel. ECL signals start to appear from 2.1 V and increase up to 2.5 V (**Figure 2**). Importantly for practical sensors, we clearly observe the ECL emissions with the naked eye at 2.2 V and larger voltage. A voltage drop along the solution over the BPE can be estimated from the ratio of the BPE length (l_{elec}) to the channel length ($l_{channel}$) in our system.

$$l_{elec} / l_{channel} = 2.2 \text{ cm} / 2.4 \text{ cm} = 0.92 \quad (3)$$

Therefore, for the overall applied voltage of 2.1 V between the two driving electrodes, the estimated voltage drop over the BPE is to be 1.932 V, which agrees well with the minimum potential (1.895 V) for ECL reactions measured in the 3-electrode system. ECL emission diminishes at a voltage larger than 2.6 V because of water oxidation on the BPE and physical damage of the BPE surface.[18]

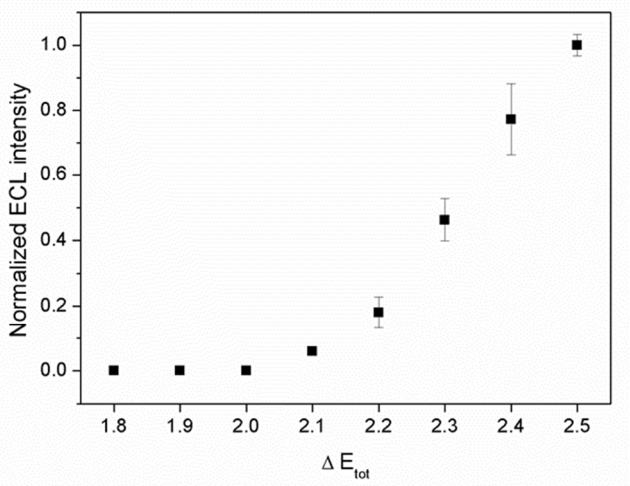

Figure 2. ECL intensities on ITO BPE as a function of applied potentials to the two driving electrodes (ΔE_{tot}). The microchannel was filled with 5 mM $Ru(bpy)_3^{2+}$ and 25 mM TPA in 0.1 M PBS solution (pH 6.9).

ECL on Bipolar Electrode Powered by RED. Prior to attaching the RED patch to the BPE microfluidic chip, we measured initial voltage of each RED patch upon injecting the

salt solutions; 1.94 ± 0.02 V, 2.50 ± 0.02 V, and 2.96 ± 0.12 V for 8-, 10-, and 12-layered RED patches, respectively (**Figure 1a**). No ECL emission is detected at the anode of the BPE with 8-layered RED patches (**Figure 3a**). Meanwhile, we observe obvious ECL emissions powered by the 10-layered RED patches where the intensity is very similar to that obtained at 2.4 V applied from the potentiostat (**Figure 2, 3b, and S6)**. This is because the RED potential continuously decreases during the exposure time of 15 s for ECL imaging by a digital camera (**Figure S5**), whereas potentiostat maintains a constant voltage of 2.4 V applied. Additionally, there is a time delay (approx. 10 s) between the voltage measurement and the ECL signal acquisition. Thus, the ECL intensities are not significantly different between the cases powered by RED and conventional electronic instrument, potentiostat, in spite of a little deviation in the potentials applied. It is safe to see ECL emissions with 12-layered RED patches. As mentioned above, however, damage of the BPE surface is possibly serious so as to cause irreproducible emission. Overall, we assure that the miniaturized RED patches can provide sufficient electric power to drive ECL reactions on the BPE.

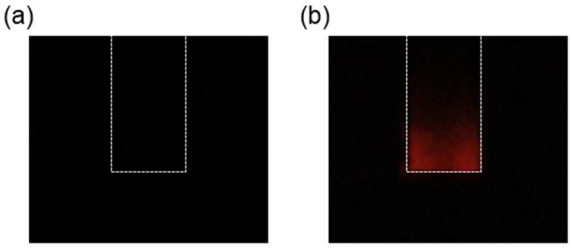

Figure 3. ECL images of $Ru(bpy)_3^{2+}$ on the BPE in the microchannel after the integration with an 8-layerd RED patch (a), and a 10-layerd RED patch (b) as a power source.

Detection of Glucose Based on RED/BPE System. We can demonstrate the functionality and applicability of RED-driven ECL system through the detection of glucose as a model analyte. We employed a solution-separated BPE system in a microfluidic chip device **(Figure 4a)**. The microchannel is separated into two parts containing different solutions while the single BPE is still contacted with the anodic and cathodic solutions.[1,11] The advantage of the closed BPE is that the analyte solution of the sensing part is physically and chemically isolated from the ECL solution of the reporting part. As a result, the oxidation and reduction reactions in those two parts can occur individually without interfering each other.[1,10,11] Furthermore, current flow along the BPE takes nearly entire current in the microchannel that is physically blocked for minimal ion transport. On the other hand, both electric current along the BPE and ion transport in the solution contribute to the overall current flow in the microchannel that is not blocked. Thus, the separated solution system can allow us to apply potential gradient over the BPE more effectively, i.e. stronger driving force for electrochemical reactions on the BPE, than the open channel system.[11]

GO_x catalyzes oxidation of glucose to produce H_2O_2, which is more readily reduced than the dissolved O_2 on the ITO surface (**Figure 4a**).[9] As the concentration of glucose increases, cathodic current increases in proportional to H_2O_2 concentration as a consequence of the catalytic reaction by GO_x. Thus, ECL intensity in the anodic part depends on glucose concentration. In order to reveal that H_2O_2 can reduce the potential required for ECL emission on the BPE sensor, we performed linear sweep voltammetry as a function of H_2O_2 concentrations in a three-electrode system. As expected, cathodic current greatly increases (**Figure S7a**) and exhibits a highly linear response in accordance with H_2O_2 concentration (R^2 = 0.99) (**Figure S7b**). When 10 mM H_2O_2 is present in PBS solution, the onset potential for the ECL reaction at ±50 μA/cm^2 is estimated to be 1.499 V, which is 0.396 V lower than the potential necessary for O_2 and water reductions, thereby demonstrating that a stronger ECL emission can be induced by means of the enzymatic reaction of GO_x depending on glucose concentration at a moderate potential.

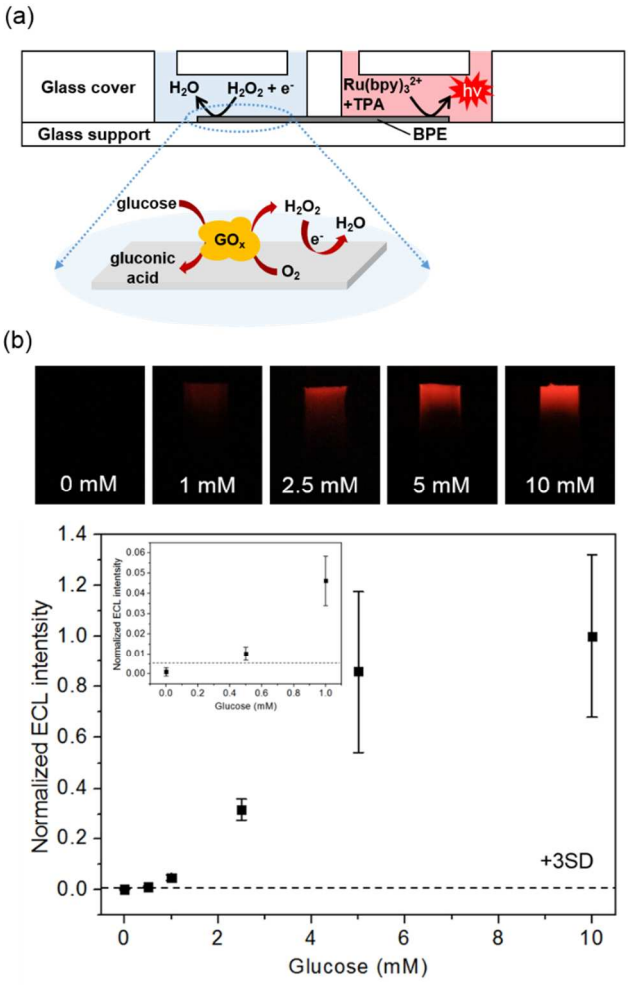

Figure 4. Schematic illustration of the closed BPE / ECL system in the microfluidic chip and the glucose sensing mechanism on the BPE (a). ECL intensities on ITO BPE as a function of the concentration of glucose when a voltage was applied by 8-layered RED (b). The error bar is the standard deviation from three independent experiments. The dashed line indicates the limit of detection determined by +3SD in the absence of glucose.

We then measured ECL intensities as a function of glucose concentration with a given concentration of GO_x (1mg/mL) using a conventional potentiostat, which was employed to hold

a constant voltage of 2.0 V between the lateral ends of microchannel. ECL intensity responds well to the concentration of glucose and its slope begin to slow down at 5 mM, whereas no emission is observed in the absence of glucose (**Figure S8**). It is assumed that the saturated ECL intensities at the two highest concentrations seem to be caused by which remaining oxygen become insufficient in the microchannel solution since the amount of dissolved oxygen is more likely to be a deficient component compared with glucose. The limit of detection (LOD) is estimated to be 0.1 mM, defined by the lowest concentration whose signal is above three-time standard deviation at the absence of glucose.

Finally, the ECL-reporting sensor was operated by the 8-layered RED patches capable of generating 1.94 ± 0.02 V. This is fairly reasonable, because if the 10-layered RED patch that produces 2.50 V is employed, oxygen reduction as well as water oxidation/reduction should be involved, rendering a background ECL emission. As expected, the RED-powered quantification of glucose worked in a similar way to the results obtained by the potentiostat (**Figure 4b**). It is notable that no ECL emission is observed with 10 mM glucose while in the absence of GO_x (**Figure S9**). When the BPE biosensor is driven by the RED patch, the LOD is 0.5 mM, which is a little higher comparing with the data obtained by the potentiostat. This is because the initial voltage of the RED is slightly lower than 2.0 V and cannot be maintained at a constant value over time. In addition, the RED-driven biosensing system in this work offers less reducible ECL responses than that by the potentiostat. The deviation in ECL intensity is ascribed to variation of initial voltage as well. Notwithstanding such the problem, it is undeniable that the miniaturized RED patch successful works as a new type of ionic power source, which is portable, easy-to-use, and eco-friendly, for biosensing operation.

CONCLUSION

We have developed the RED-powered electrochemical sensing device based on ECL/BPE system for the first time. Disposable miniaturized RED patches were specifically designed and fabricated for appropriate combination with ECL reporting in the microfluidic system. We found that voltage demanded for electrochemical sensing operations can be readily obtained by adjusting a salinity ratio and the number of IEMs. In addition, the easy-to-use, eco-friendly and biocompatible characteristics of the RED patches can augment practical values of various analytical devices that require low electrical power for their operations. In spite of attractive capabilities as a new power source, there still remain tasks for practical uses in the third or developing countries. To name a few, simpler way for injecting salt solutions and alternative materials cheaper than commercial IEMs and electrodes (e.g. paper-based ion-selective membranes or electrodes) are necessary for cost-effective manufacturing.[9,19-22] With subsequent effort for advance, it is expected that the eco-friendly portable RED-powered electrochemical sensing system might be emerging as the stereotype of disposable battery-free biosensors for the practical applications in the near future.

ASSOCIATED CONTENT

Supporting Information

The Supporting Information is available free of charge on the ACS Publications website.
Schematic design of RED patches, real images of RED patches combined with microfluidic chips, measurement method of microchannel resistance, electrochemical behavior of $Ru(bpy)_3^{2+}$/TPA obtained in three-electrode system, potential behavior of RED patches, comparison of ECL intensities obtained by potentiostat and RED, and additional information about glucose sensing (PDF)

AUTHOR INFORMATION

Corresponding Author

* Tel.: +82-2-880-4362. Fax: +82-2-887-4354. E-mail: tdchung@snu.ac.kr.

Author Contributions

The manuscript was written through contributions of all authors. / All authors have given approval to the final version of the manuscript. / ‡These authors contributed equally.

ACKNOWLEDGMENTS

This research was supported by Nano. Material Technology Development Program through the National Research Foundation of Korea (NRF) funded by the Ministry of Science, ICT and Future Planning (2011-0030268), CABMC (Control of Animal Brain using MEMS Chip) funded by Defense Acquisition Program Administration (UD140069ID), and the National Research Foundation of Korea(NRF) grant funded by the Korea government(MSIP) (No. 2015R1A2A1A13001897).

REFERENCES

(1) Fosdick, S. E.; Knust, K. N.; Scida, K.; Crooks, R. M. *Angew. Chem. Int. Ed.* **2013**, *52*, 10438-10456.
(2) Bradley, J.-C.; Chen, H.-M.; Crawford, J.; Eckert, J.; Ernazarova, K.; Kurzeja, T.; Lin, M.; McGee, M.; Nadler, W.; Stephens, S. G. *Nature* **1997**, *389*, 268-271.
(3) Chow, K.-F.; Mavré, F.; Crooks, R. M. *J. Am. Chem. Soc.* **2008**, *130*, 7544-7545.
(4) Fosdick, S. E.; Crooks, R. M. *J. Am. Chem. Soc.* **2012**, *134*, 863-866.
(5) Hlushkou, D.; Perdue, R. K.; Dhopeshwarkar, R.; Crooks, R. M.; Tallarek, U. *Lab on a Chip* **2009**, *9*, 1903-1913.
(6) Laws, D. R.; Hlushkou, D.; Perdue, R. K.; Tallarek, U.; Crooks, R. M. *Anal. Chem.* **2009**, *81*, 8923-8929.
(7) Zhan, W.; Alvarez, J.; Crooks, R. M. *J. Am. Chem. Soc.* **2002**, *124*, 13265-13270.
(8) Wu, M.-S.; Yuan, D.-J.; Xu, J.-J.; Chen, H.-Y. *Chem. Sci.* **2013**, *4*, 1182-1188.
(9) Feng, Q.-M.; Pan, J.-B.; Zhang, H.-R.; Xu, J.-J.; Chen, H.-Y. *Chem. Commun.* **2014**, *50*, 10949-10951.
(10) Zhang, X.; Li, J.; Jia, X.; Li, D.; Wang, E. *Anal. Chem.* **2014**, *86*, 5595-5599.
(11) Wu, M.-S.; Liu, Z.; Shi, H.-W.; Chen, H.-Y.; Xu, J.-J. *Anal. Chem.* **2015**, *87*, 530-537.
(12) Chen, L.; Zhang, C.; Xing, D. *Sens. Actuators, B* **2016**, *237*, 308-317.
(13) Post, J. W.; Hamelers, H. V.; Buisman, C. *J. Environ. Sci. Technol.* **2008**, *42*, 5785-5790.
(14) Arora, A.; Eijkel, J. C.; Morf, W. E.; Manz, A. *Anal. Chem.* **2001**, *73*, 3282-3288.
(15) Lin, C.-H.; Lee, G.-B.; Lin, Y.-H.; Chang, G.-L. *J. Micromech. Microeng.* **2001**, *11*, 726.
(16) Długołęcki, P.; Nymeijer, K.; Metz, S.; Wessling, M. *J. Membr. Sci.* **2008**, *319*, 214-222.
(17) Mavré, F. o.; Chow, K.-F.; Sheridan, E.; Chang, B.-Y.; Crooks, J. A.; Crooks, R. M. *Anal. Chem.* **2009**, *81*, 6218-6225.
(18) Zu, Y.; Bard, A. J. *Anal. Chem.* **2000**, *72*, 3223-3232.

(19) Novell, M.; Parrilla, M.; Crespo, G. n. A.; Rius, F. X.; Andrade, F. J. *Anal. Chem.* **2012**, *84*, 4695-4702.
(20) Costa, M.; Veigas, B.; Jacob, J.; Santos, D.; Gomes, J.; Baptista, P.; Martins, R.; Inácio, J.; Fortunato, E. *Nanotechnology* **2014**, *25*, 094006.
(21) Lan, W.-J.; Zou, X. U.; Hamedi, M. M.; Hu, J.; Parolo, C.; Maxwell, E. J.; Bühlmann, P.; Whitesides, G. M. *Anal. Chem.* **2014**, *86*, 9548-9553.
(22) Mensah, S. T.; Gonzalez, Y.; Calvo-Marzal, P.; Chumbimuni-Torres, K. Y. *Anal. Chem.* **2014**, *86*, 7269-7273.

For Table of Contents Only